

# Chiral SU(3) dynamics and $\Lambda$ hyperons in the nuclear medium

N. Kaiser and W. Weise

*Physik-Department, Technische Universität München, D-85747 Garching, Germany*

(Received 14 October 2004; published 19 January 2005)

We present a novel approach to the density-dependent mean field and the spin-orbit interaction of a  $\Lambda$  hyperon in a nuclear many-body system, based on flavor-SU(3) in-medium chiral perturbation theory. The leading long-range  $\Lambda N$  interaction arises from kaon exchange and from two-pion exchange with a  $\Sigma$  hyperon in the intermediate state. The empirical  $\Lambda$ -nucleus potential depth of about  $-28$  MeV is well reproduced with a single cutoff scale,  $\bar{\Lambda} = 0.7$  GeV, effectively representing all short-distance (high-momentum) dynamics not resolved at scales characteristic of the nuclear Fermi momentum. This value of  $\bar{\Lambda}$  is remarkably consistent with the one required to reproduce the empirical saturation point of isospin-symmetric nuclear matter in the same framework. The smallness of the  $\Lambda$ -nuclear spin-orbit interaction finds a natural (yet novel) explanation in terms of an almost complete cancellation between short-range contributions (properly rescaled from the known nucleonic spin-orbit coupling strength) and long-range terms generated by iterated one pion exchange with intermediate  $\Sigma$  hyperons. The small  $\Sigma\Lambda$ -mass difference figures prominently in this context.

DOI: 10.1103/PhysRevC.71.015203

PACS number(s): 21.80.+a, 13.75.Ev, 21.65.+f, 24.10.Cn

## I. INTRODUCTION AND FRAMEWORK

The physics of  $\Lambda$  hypernuclei has a long and well-documented history [1–4]. It has at the same time raised questions of fundamental interest. The empirical single-particle energies of a  $\Lambda$  hyperon bound in hypernuclei are well described in terms of an attractive mean-field about half as strong as the one for nucleons in nuclei [2]. In contrast, the extraordinary weakness of the  $\Lambda$ -nucleus spin-orbit interaction, as compared to the one in ordinary nuclei, has always been a puzzle. For example, recent precision measurements [5] of  $E1$ -transitions from  $p$ - to  $s$ -shell orbitals of a  $\Lambda$  hyperon in  ${}^{13}_{\Lambda}\text{C}$  give a  $p_{3/2} - p_{1/2}$  spin-orbit splitting of only  $(152 \pm 65)$  keV to be compared with about 6 MeV in ordinary  $p$ -shell nuclei. Even admitting a large uncertainty in the hypernuclear case, the  $\Lambda$ -nuclear spin-orbit interaction appears to be systematically weaker by at least an order of magnitude than the  $N$ -nucleus spin-orbit force.

Over the years, various attempts have been made to understand this phenomenon [6–8]. So far, standard calculations using one-boson exchange  $\Lambda N$  potentials [9–12] tend to overestimate the  $\Lambda$ -nucleus spin-orbit splittings significantly. SU(3) generalizations of standard nuclear relativistic mean-field models, such as the one reported in Ref. [13], require extra parameters to deal with the spin-orbit problem. The importance of  $\Lambda$ - $\Sigma^0$  mixing in the context of SU(3) effective Lagrangians applied to  $\Lambda$ -hypernuclei has been emphasized in Ref. [14]. The small spin-orbit coupling of the  $\Lambda$  hyperon emerges naturally in the naive SU(6) quark model with flavor symmetry breaking. An approach that combines quark model aspects with scalar and vector meson exchange (the quark-meson coupling model) has also been applied to hypernuclei [15], with Pauli blocking in the  $\Lambda N$ - $\Sigma N$  coupled channels incorporated phenomenologically. Another option that has been studied at the quark level is the color analog of the Fermi-Breit interaction within a resonating-group approach [16], albeit with a large quark-gluon coupling outside the range of perturbative applicability.

More recently, in-medium effective field theory approaches have opened new perspectives for dealing with the issues of single-particle motion and spin-orbit coupling in ordinary nuclei, both symmetric and asymmetric in isospin. In this work we take steps toward including strangeness in such a framework.

Our calculation is based on the leading order chiral meson-baryon Lagrangian in flavor-SU(3):

$$\mathcal{L}_{\phi B} = \text{tr}(\bar{B}(\gamma_{\mu}(i\partial^{\mu}B + [\Gamma^{\mu}, B]) - M_B)B) + D \text{tr}(\bar{B}\gamma_{\mu}\gamma_5\{u^{\mu}, B\}) + F \text{tr}(\bar{B}\gamma_{\mu}\gamma_5[u^{\mu}, B]), \quad (1)$$

where the traceless hermitian  $3 \times 3$  matrix  $B$  of Dirac spinors represents the octet baryon fields ( $N$ ,  $\Lambda$ ,  $\Sigma$ ,  $\Xi$ ) with mass  $M_B$ . The chiral connection  $\Gamma^{\mu} = i[\xi^{\dagger}, \partial^{\mu}\xi]/2$  and the axial-vector quantity  $u^{\mu} = i\{\xi^{\dagger}, \partial^{\mu}\xi\}/2$  generate interaction terms with the Goldstone bosons ( $\pi$ ,  $K$ ,  $\bar{K}$ ,  $\eta$ ) collected in the SU(3) matrix  $\xi = \exp(i\phi/2f)$ . The parameter  $f$  is identified with the weak pion decay constant  $f_{\pi} = 92.4$  MeV and  $D$  and  $F$  denote the SU(3) axial-vector coupling constants of the baryons. We choose as their values  $D = 0.84$  and  $F = 0.46$ . This leads to a  $KN\Lambda$ -coupling constant of  $g_{KN\Lambda} = (D + 3F)(M_N + M_{\Lambda})/(2\sqrt{3}f_{\pi}) = 14.25$  and a  $\pi\Lambda\Sigma$ -coupling constant of  $g_{\pi\Lambda\Sigma} = D(M_{\Lambda} + M_{\Sigma})/(\sqrt{3}f_{\pi}) = 12.12$ , which are both consistent with the empirical values summarized in Tables 6.3 and 6.4 of Ref. [17]. Our  $KN\Lambda$ -coupling constant is compatible with the upper range of the interval given for  $g_{KN\Lambda}$  in the recent systematic compilation of Ref. [18]. The  $\pi\Lambda\Sigma$ -coupling constant used in the present work is consistent with the one extracted from hyperonic atoms [19]. Furthermore, the pion-nucleon coupling constant has the value  $g_{\pi N} = g_A M_N/f_{\pi} = 13.2$  with  $g_A = D + F = 1.3$ . Apart from these three pseudovector  $KN\Lambda$ ,  $\pi\Lambda\Sigma$ , and  $\pi NN$  couplings, no further interaction terms from  $\mathcal{L}_{\phi B}$  come into play to the order we are working here.

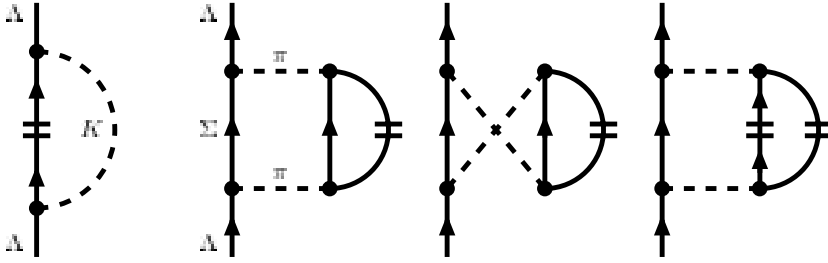


FIG. 1. One-kaon exchange Fock diagram and two-pion exchange Hartree diagrams with  $\Sigma$  hyperons in the intermediate state. The horizontal double lines represent the filled Fermi sea of nucleons in the in-medium nucleon propagator,  $(\gamma \cdot p - M_N)[i(p^2 - M_N^2 + i\epsilon)^{-1} - 2\pi\delta(p^2 - M_N^2)\theta(p_0)\theta(k_f - |\vec{p}|)]$ . The isospin factors of the kaon- and pion-exchange diagrams are 2 and 6, respectively.

## II. $\Lambda$ -NUCLEUS SINGLE-PARTICLE POTENTIAL

Consider first the density-dependent mean-field  $U_\Lambda(k_f)$  for a zero-momentum  $\Lambda$  hyperon placed as a test particle in isospin-symmetric nuclear matter. The potential depth  $U_\Lambda(k_{f0})$  at equilibrium density  $\rho_0 = 0.16 \text{ fm}^{-3}$  determines primarily the spectra of medium heavy and heavy  $\Lambda$  hypernuclei. We calculate the long-range contributions generated by the exchange of light Goldstone bosons between the  $\Lambda$  hyperon and the nucleons in the filled Fermi sea. The only nonvanishing one-meson exchange contribution comes from the kaon-exchange Fock diagram in Fig. 1, from which we obtain the following repulsive contribution to the  $\Lambda$ -nuclear mean field:

$$U_\Lambda(k_f)^{(K)} = \frac{(D + 3F)^2}{(6\pi f_\pi)^2} \left\{ k_f^3 - 3m_K^2 k_f + 3m_K^3 \arctan \frac{k_f}{m_K} \right\} + \mathcal{O}(M_B^{-2}), \quad (2)$$

with  $m_K = 496 \text{ MeV}$  the average kaon mass. At densities at and below nuclear matter saturation density  $\rho \leq 0.16 \text{ fm}^{-3}$  (corresponding to Fermi momenta  $k_f \leq 263 \text{ MeV}$ ) the one-kaon exchange can already be regarded as being of short range. The ratio  $k_f/m_K \leq 0.53$  is small and the expression in curly brackets of Eq. (2) is dominated by its leading term  $3k_f^3/5m_K^2$  in the  $k_f$  expansion.

Because one-pion exchange is excluded by isospin invariance, the leading long-range interaction between the  $\Lambda$ -hyperon and the nucleons arises from two-pion exchange. The corresponding two-loop diagrams with a  $\Sigma$  hyperon in the intermediate state are shown in Fig. 1. The small  $\Sigma\Lambda$ -mass splitting  $M_\Sigma - M_\Lambda = 77.5 \text{ MeV}$  that comes into play here is comparable in magnitude to  $k_{f0}^2/M_N$ , twice the typical kinetic energies of the nucleons. Therefore it has to be counted accordingly in the energy denominator. Putting all pieces together we find from the second diagram in Fig. 1 the following attractive contribution to the  $\Lambda$ -nuclear mean field:

$$U_\Lambda(k_f)^{(2\pi)} = -\frac{D^2 g_A^2}{f_\pi^4} \int_{|\vec{p}_1| < k_f} \frac{d^3 p_1 d^3 l}{(2\pi)^6} \times \frac{M_B \bar{l}^4}{(m_\pi^2 + \bar{l}^2)^2 [\Delta^2 + \bar{l}^2 - \vec{l} \cdot \vec{p}_1]} + \mathcal{O}(M_B^{-1}), \quad (3)$$

with  $m_\pi = 138 \text{ MeV}$  the average pion mass. The mean baryon mass  $M_B = (2M_N + M_\Lambda + M_\Sigma)/4 = 1047 \text{ MeV}$  serves the purpose of averaging out differences in the kinetic energies

of the various baryons involved. The relation  $M_\Sigma - M_\Lambda = \Delta^2/M_B$  for the  $\Sigma\Lambda$ -mass splitting defines another small mass scale  $\Delta$ . Its magnitude  $\Delta \simeq 285 \text{ MeV}$  is close to the Fermi momentum  $k_{f0} = 263 \text{ MeV}$  at saturation density. As it stands the  $d^3 l$ -loop integral in Eq. (3) is ultraviolet divergent. By subtracting  $M_B/\bar{l}^2$  from the integrand it becomes convergent and analytically solvable. After regularizing the remaining (structureless) linear divergence  $\int_0^\infty dl$  by a momentum cutoff  $\bar{\Lambda}$  we get

$$U_\Lambda(k_f)^{(2\pi)} = \frac{D^2 g_A^2 M_B}{(2\pi f_\pi)^4} \left\{ -\frac{4\bar{\Lambda}}{3} k_f^3 + \pi m_\pi^3 k_f \Phi\left(\frac{k_f^2}{m_\pi^2}, \frac{\Delta^2}{m_\pi^2}\right) \right\} + \mathcal{O}(M_B^{-1}), \quad (4)$$

with the function

$$\Phi(u, \delta) = \delta - 3 + \frac{1}{4}(u - 2\delta + 6)\sqrt{4\delta - u} + \frac{2}{\sqrt{u}}(2u + \delta^2 - 4\delta + 3) \arctan \frac{\sqrt{u}}{2 + \sqrt{4\delta - u}}, \quad (5)$$

emerging from the combined loop and Fermi-sphere integration, where  $u = k_f^2/m_\pi^2$  and  $\delta = \Delta^2/m_\pi^2$ . The branch point of the function  $\Phi(u, \delta)$  at  $k_f = 2\Delta$  is related to the kinematical threshold for the (on-shell) scattering process  $\Lambda N \rightarrow \Sigma N$ . This threshold is reached only at very high densities,  $\rho \geq 1.4 \text{ fm}^{-3}$ . Note that the decomposition in Eq. (4) is optimal from the point of view of separating effects from high and low mass scales. The (high-momentum) cutoff scale  $\bar{\Lambda}$  effectively parameterizes the strength of an attractive  $\Lambda N$ -contact interaction. No dependence on the two low-mass scales,  $m_\pi$  and  $\Delta$ , is left over in the corresponding term linear in the nucleon density  $\rho = 2k_f^3/3\pi^2$ . The third diagram in Fig. 1 with crossed pion lines corresponds to irreducible two-pion exchange between the  $\Lambda$  hyperon and the nucleons. At leading order in the small momentum expansion it is exactly canceled by a  $M_B$ -independent contribution from the second diagram in Fig. 1 (with parallel pion lines). Note that the same exact cancellation between the planar and crossed box graphs is at work in the isoscalar central channel of the  $2\pi$ -exchange  $NN$  potential (for details see Sec. 4.2 in Ref. [20]). Thus we are left with the Pauli-blocking correction to the iterated pion-exchange diagram with intermediate  $\Sigma$  states. From the last diagram in Fig. 1 we find the following repulsive contribution to the  $\Lambda$ -nuclear mean field:

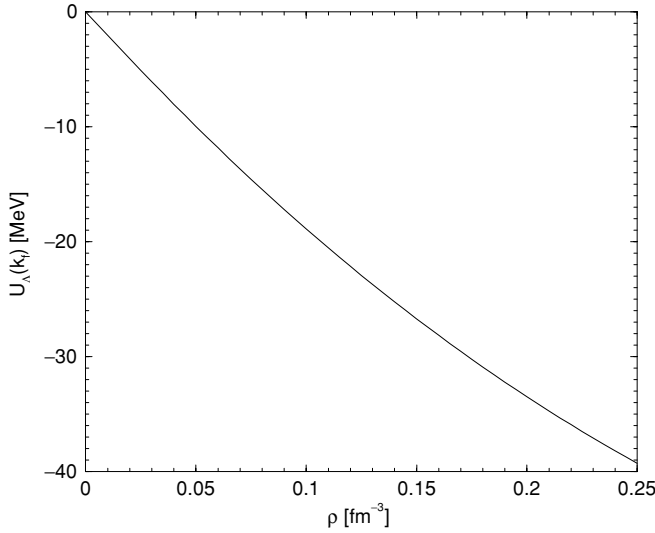


FIG. 2. The mean-field  $U_\Lambda(k_f)$  of a  $\Lambda$  hyperon in isospin-symmetric nuclear matter versus the nucleon density  $\rho = 2k_f^3/3\pi^2$ . The cutoff scale  $\bar{\Lambda}$  has been adjusted to the value  $\bar{\Lambda} = 0.70$  GeV.

$$U_\Lambda(k_f)_{\text{med}}^{(2\pi)} = \frac{D^2 g_A^2}{f_\pi^4} \int_{|\vec{p}_{1,2}| < k_f} \frac{d^3 p_1 d^3 p_2}{(2\pi)^6} \times \frac{M_B (\vec{p}_1 - \vec{p}_2)^4}{[m_\pi^2 + (\vec{p}_1 - \vec{p}_2)^2]^2 [\Delta^2 + \vec{p}_2^2 - \vec{p}_1 \cdot \vec{p}_2]} + \mathcal{O}(M_B^{-1}). \quad (6)$$

After performing the angular integrations this expression reduces to an easily manageable two-dimensional integral:

$$U_\Lambda(k_f)_{\text{med}}^{(2\pi)} = \frac{D^2 g_A^2 M_B m_\pi^4}{2(2\pi f_\pi)^4} \int_0^u dx \int_0^u dy \frac{1}{(2\delta - 1 - x + y)^2} \times \left\{ \frac{4(2\delta - 1 - x + y)\sqrt{xy}}{(1 + x + y)^2 - 4xy} + (2x - 2y - 4\delta + 1) \ln \frac{1 + x + y + 2\sqrt{xy}}{1 + x + y - 2\sqrt{xy}} + (2\delta - x + y)^2 \ln \frac{\delta + y + \sqrt{xy}}{\delta + y - \sqrt{xy}} \right\}, \quad (7)$$

with the abbreviations  $u = k_f^2/m_\pi^2$  and  $\delta = \Delta^2/m_\pi^2$ .

Summing up all terms, Fig. 2 shows the calculated  $\Lambda$ -nuclear mean-field  $U_\Lambda(k_f)$  as a function of the nucleon density  $\rho = 2k_f^3/3\pi^2$ . The cutoff scale has been adjusted to the value  $\bar{\Lambda} = 0.7$  GeV. At normal nuclear matter density  $\rho_0 = 0.16 \text{ fm}^{-3}$  (corresponding to  $k_{f0} = 263 \text{ MeV}$ ) one finds  $U_\Lambda(k_{f0}) = (4.17 - 39.77 + 7.46) \text{ MeV} = -28.15 \text{ MeV}$ , where the individual entries correspond to one-kaon exchange, iterated one-pion exchange with intermediate  $\Sigma N$  states, and the Pauli-blocking correction to the latter. Note that the physically reasonable cutoff scale  $\bar{\Lambda} = 0.70$  GeV which reproduces the empirical potential depth  $U_\Lambda(k_{f0}) \simeq -28 \text{ MeV}$  [1] is close to  $\bar{\Lambda} = 0.65$  GeV needed to reproduce the empirical saturation point of isospin-symmetric nuclear matter in the same framework [21]. This is a remarkable and nontrivial

feature. At the present stage of our calculation all other possible contributions to the  $\Lambda$ -nuclear mean-field  $U_\Lambda(k_f)$  from  $\pi K$  exchange,  $\bar{K} K$  exchange, and so on, are hidden in the adjusted value of the cutoff  $\bar{\Lambda} = 0.70$  GeV, or equivalently, in the contact term that encodes short-distance dynamics not resolved at momentum scales around  $k_{f0}$ . At the densities of interest all those effects can be regarded as being of short range nature and therefore they are summarized by this single term linear in the nucleon density  $\rho = 2k_f^3/3\pi^2$ .

### III. $\Lambda$ -NUCLEUS SPIN-ORBIT INTERACTION

The empirical finding that the  $\Lambda$ -nucleus spin-orbit coupling is negligibly small in comparison to the strong spin-orbit interaction of nucleons in ordinary nuclei presents an outstanding problem in low-energy hadron physics. In relativistic scalar-vector mean-field models a strong tensor coupling of the  $\omega$  meson to the  $\Lambda$  hyperon, equal and of opposite sign to the vector-coupling, has been proposed as a possible solution [8]. We demonstrate here that there is a more natural source of cancellation in the hypernuclear many-body problem.

The pertinent quantity to extract the  $\Lambda$ -nuclear spin-orbit coupling is the spin-dependent part of the self-energy of a  $\Lambda$  hyperon interacting with weakly inhomogeneous isospin-symmetric nuclear matter. Let the  $\Lambda$ -hyperon scatter from initial momentum  $\vec{p} - \vec{q}/2$  to final momentum  $\vec{p} + \vec{q}/2$ . The spin-orbit part of the self-energy in the weakly inhomogeneous medium is then [22]

$$\Sigma_{\text{spin}} = \frac{i}{2} \vec{\sigma} \cdot (\vec{q} \times \vec{p}) U_{\Lambda ls}(k_f), \quad (8)$$

where the density-dependent spin-orbit coupling strength  $U_{\Lambda ls}(k_f)$  is taken in the limit of homogeneous nuclear matter (characterized by its Fermi momentum  $k_f$ ) and zero external  $\Lambda$ -momenta:  $\vec{p} = \vec{q} = 0$ . The more familiar spin-orbit Hamiltonian of the shell model follows from Eq. (8) by multiplication with a density form factor and Fourier transformation:

$$\mathcal{H}_{\Lambda ls} = U_{\Lambda ls}(k_{f0}) \frac{1}{2r} \frac{df(r)}{dr} \vec{\sigma} \cdot \vec{L}. \quad (9)$$

Here  $f(r)$  is the normalized nuclear density profile with  $f(0) = 1$ , and  $\vec{L} = \vec{r} \times \vec{p}$  is the orbital angular momentum. For reference and orientation, consider first the frequently used simple model of isoscalar vector boson ( $\omega$ -meson) exchange between the  $\Lambda$  hyperon and the nucleon. The nonrelativistic expansion of the vector (and tensor) coupling vertex between Dirac spinors of the  $\Lambda$  hyperon gives rise to a spin-orbit term proportional to  $i \vec{\sigma} \cdot (\vec{q} \times \vec{p})/4M_\Lambda^2$ . Next one takes the limit of homogeneous nuclear matter (i.e.  $\vec{q} = 0$ ), performs the remaining integral over the nuclear Fermi sphere and arrives at the familiar result:

$$U_{\Lambda ls}(k_f)^{(\omega)} = \frac{G_V}{2M_\Lambda^2} \rho, \quad (10)$$

linear in the nucleon density  $\rho$ . Here,  $G_V = g_{\omega\Lambda}(1 + 2\kappa_{\omega\Lambda})g_{\omega N}/m_\omega^2$  is a coupling strength of dimension (length)<sup>2</sup>, which includes the  $\omega$ -baryon coupling constants, a possible tensor coupling of the  $\omega$  meson to the  $\Lambda$  hyperon with  $\kappa_{\omega\Lambda}$

the tensor-to-vector coupling ratio, and the  $\omega$ -meson mass  $m_\omega$ . In the absence of  $\kappa_{\omega\Lambda}$  and assuming that the  $\omega$  meson does not couple to the strange quark in the  $\Lambda$  hyperon, one would naively expect  $G_V$  to be  $2/3$  of the corresponding piece of the  $NN$  interaction for which  $G_V \simeq 12 \text{ fm}^2$ . Evidently, an almost vanishing  $\Lambda$ -nuclear spin-orbit force would be difficult to understand at this stage unless one postulates a much reduced coupling  $g_{\omega\Lambda}$  or a sizeable and negative tensor-to-vector coupling ratio  $\kappa_{\omega\Lambda}$  [8].

The important observation is now that iterated one-pion exchange with an intermediate  $\Sigma$  hyperon also generates a sizeable spin-orbit coupling, with a sign opposite to that expected from the short-range interactions. The prefactor  $i \vec{\sigma} \times \vec{q}$  is immediately identified by rewriting the product of  $\pi\Lambda\Sigma$ -interaction vertices  $\vec{\sigma} \cdot (\vec{l} - \vec{q}/2) \vec{\sigma} \cdot (\vec{l} + \vec{q}/2)$  at the open baryon line in the  $2\pi$ -exchange process shown by the second diagram in Fig. 1. For all remaining parts of the iterated pion-exchange diagram one can then take the limit of homogeneous nuclear matter (i.e.,  $\vec{q} = 0$ ). The other essential factor  $\vec{p}$  emerges from the energy denominator  $\Delta^2 + \vec{l} \cdot (\vec{l} - \vec{p}_1 + \vec{p})$ . Keeping only the term linear in the external momentum  $\vec{p}$  one finds from the second diagram in Fig. 1 the following contribution to the  $\Lambda$ -nuclear spin-orbit coupling strength:

$$U_{\Lambda s}(k_f)^{(2\pi)} = -\frac{2D^2 g_A^2}{3f_\pi^4} \int_{|\vec{p}_1| < k_f} \frac{d^3 p_1 d^3 l}{(2\pi)^6} \times \frac{M_B \vec{l}^4}{(m_\pi^2 + \vec{l}^2)^2 [\Delta^2 + \vec{l}^2 - \vec{l} \cdot \vec{p}_1]^2}. \quad (11)$$

This loop integral is convergent as it stands. It can be solved together with the Fermi sphere integral in closed form:

$$U_{\Lambda s}(k_f)^{(2\pi)} = \frac{D^2 g_A^2 M_B m_\pi k_f}{24\pi^3 f_\pi^4} \Omega\left(\frac{k_f^2}{m_\pi^2}, \frac{\Delta^2}{m_\pi^2}\right), \quad (12)$$

with the function:

$$\Omega(u, \delta) = \frac{1}{u + (\delta - 1)^2} [6\delta - 2\delta^2 - 4 - 3u + (\delta^2 - 3\delta + 2 + u)\sqrt{4\delta - u}] + \frac{4}{\sqrt{u}} (2 - \delta) \arctan \frac{\sqrt{u}}{2 + \sqrt{4\delta - u}}. \quad (13)$$

The Pauli-blocking correction to the  $\Lambda$ -nuclear spin-orbit coupling strength generated by iterated pion exchange is calculated in the same way:

$$U_{\Lambda s}(k_f)_{\text{med}}^{(2\pi)} = \frac{2D^2 g_A^2}{3f_\pi^4} \int_{|\vec{p}_{1,2}| < k_f} \frac{d^3 p_1 d^3 p_2}{(2\pi)^6} \times \frac{M_B (\vec{p}_1 - \vec{p}_2)^4}{[m_\pi^2 + (\vec{p}_1 - \vec{p}_2)^2]^2 [\Delta^2 + \vec{p}_2^2 - \vec{p}_1 \cdot \vec{p}_2]^2}, \quad (14)$$

and after performing the angular integrations it turns into the numerically easily manageable form:

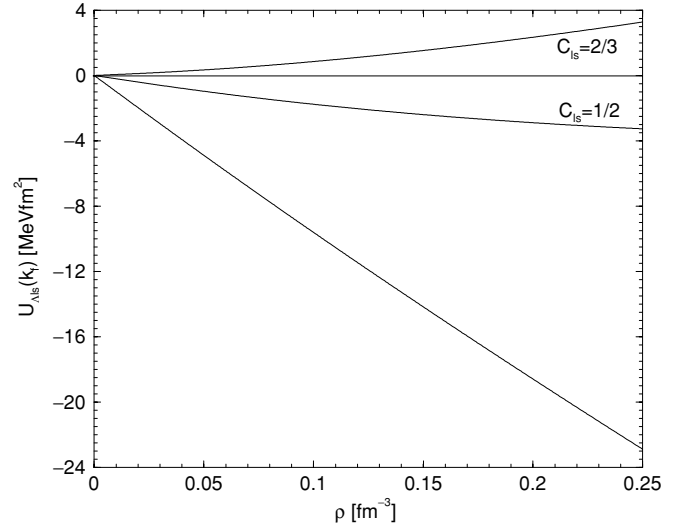


FIG. 3. The spin-orbit coupling strength  $U_{\Lambda s}(k_f)$  of a  $\Lambda$  hyperon in isospin-symmetric nuclear matter versus the nucleon density  $\rho = 2k_f^3/3\pi^2$ . The lower curve shows the long-range contribution from iterated  $1\pi$  exchange with  $\Sigma$  hyperons in the intermediate state. The two upper curves include in addition the short-range contribution,  $U_{\Lambda s}(k_f)^{(\text{sh})} = 24.8 C_{ls} \text{ MeV fm}^2 \cdot \rho/\rho_0$ , with  $C_{ls} = 2/3$  and  $1/2$ .

$$U_{\Lambda s}(k_f)_{\text{med}}^{(2\pi)} = \frac{D^2 g_A^2 M_B m_\pi^2}{12(\pi f_\pi)^4} \int_0^u dx \int_0^u dy \times \frac{1}{(2\delta - 1 - x + y)^2} \left\{ \frac{2\sqrt{xy}}{(1+x+y)^2 - 4xy} + \frac{(2\delta - x + y)^2 \sqrt{xy}}{2(\delta + y)^2 - 2xy} + \frac{2\delta - x + y}{2\delta - 1 - x + y} \times \ln \frac{(\delta + y + \sqrt{xy})(1 + x + y - 2\sqrt{xy})}{(\delta + y - \sqrt{xy})(1 + x + y + 2\sqrt{xy})} \right\}. \quad (15)$$

The two terms, Eqs. (12) and (15), are model independent in the sense that they require no regularization. Their input parameters (couplings constants and masses) are physical quantities and thus uniquely fixed. Note that these spin-orbit couplings are not relativistic effects: they are even proportional to the baryon mass  $M_B$ . This large scale enhancement factor originates from the energy denominator of the iterated pion-exchange diagram. The expressions in Eqs. (12) and (15) constitute the unique long-range  $\Lambda$ -nuclear spin-orbit interaction. The summed contributions from these  $2\pi$ -exchange processes are shown by the lower solid line in Fig. 3. They are of comparable magnitude but of opposite sign with respect to the short-range pieces mentioned earlier. The short-range part of the  $\Lambda$ -nuclear spin-orbit interaction results from a variety of processes, one of them being the isoscalar-vector exchange piece discussed previously. We relate the short-distance spin-orbit coupling of the  $\Lambda$  hyperon to the corresponding one of the nucleon as follows:

$$U_{\Lambda s}(k_f)^{(\text{sh})} = C_{ls} \frac{M_N^2}{M_\Lambda^2} U_{Ns}(k_f)^{(\text{sh})}. \quad (16)$$



The factor  $(M_N/M_\Lambda)^2$  results from the replacement of the nucleon by a  $\Lambda$ -hyperon in these relativistic spin-orbit terms. The coefficient  $C_{ls}$  parameterizes the ratio of the relevant coupling strengths. The upper limit expected from naive quark model considerations is  $C_{ls} = 2/3$ . Estimates from a QCD sum rule analysis of the Lorentz scalar and vector mean fields of a  $\Lambda$  hyperon in a nuclear medium [23] indicate that  $C_{ls}$  is smaller than its naive quark model value, partly as consequence of flavor-SU(3) breaking. For nucleons in nuclei, large Lorentz scalar and vector mean fields with their in-medium behavior governed by QCD sum rules can explain the strong spin-orbit coupling in calculations that combine these mean-fields with the long- and intermediate-range attraction provided by perturbative chiral pion-nucleon dynamics [24]. Consider now the leading terms of the vector self-energies  $\Sigma_V$ , linear in the quark density  $\langle u^\dagger u \rangle = \langle d^\dagger d \rangle = 3\rho/2$ , in a nuclear medium with only  $u$  and  $d$  quarks. From Ref. [23] one estimates roughly  $\Sigma_V(\Lambda)/\Sigma_V(N) \simeq 1/2$  for the ratio of vector mean fields experienced by a  $\Lambda$  hyperon and a nucleon. Corrections from in-medium condensates of higher dimension tend to reduce this ratio further. For the Lorentz scalar mean fields, the QCD sum rule results are subject to larger uncertainties due to the unknown contributions from four-quark condensates. Conversely, at least some of these contributions are accounted for by our explicit treatment of two-pion exchange processes. We therefore assume as a reasonable estimate, guided by [23], a factor  $C_{ls} \simeq 0.4$ – $0.5$  for both the scalar and vector self-energies that act coherently to produce the short-range spin-orbit force and cancel in the spin-averaged single-particle potential  $U_\Lambda(k_f)$ . In practice, we shall vary  $C_{ls}$  between  $1/2$  and  $2/3$ .

For the further discussion we take the value  $U_{Nls}(k_{f0})^{(sh)} = 35 \text{ MeV fm}^2$  of the nucleonic spin-orbit coupling strength from shell model calculations [25]. Phenomenological Skyrme forces [26] give approximately the same value  $U_{Nls}(k_{f0})^{(sh)} = 3\rho_0 W_0/2 \simeq 30 \text{ MeV fm}^2$  (with  $W_0 = 124 \text{ MeV fm}^5$  the spin-orbit parameter in the Skyrme phenomenology). The lower curve in Fig. 3 shows the  $\Lambda$ -nuclear spin-orbit coupling strength generated by iterated pion exchange with  $\Sigma$  hyperons in the intermediate state as a function of the nucleon density  $\rho = 2k_f^3/3\pi^2$ . The upper curves include in addition the short-range contribution  $U_{\Lambda ls}(k_f)^{(sh)} = 24.8 C_{ls} \text{ MeV fm}^2 \cdot \rho/\rho_0$ , which is obtained via Eq. (16) from the empirical nucleonic spin-orbit coupling strength with  $C_{ls}$  taken at the values  $2/3$  and  $1/2$ . At nuclear matter saturation density  $\rho_0 = 0.16 \text{ fm}^{-3}$  one finds  $U_{\Lambda ls}(k_{f0}) = (24.8 C_{ls} - 16.70 + 1.64) \text{ MeV fm}^2$ , where the individual entries correspond to the short-range term, the contribution from iterated  $1\pi$ -exchange and the Pauli-blocking correction to the latter. One observes a strong cancellation between the short- and long-range contributions. This so-far unnoticed balance between sizeable “correct-sign” and “wrong-sign” spin-orbit terms for the  $\Lambda$  hyperon offers a novel and natural explanation for the empirically observed small spin-orbit splittings in  $\Lambda$  hypernuclei, although with still persisting uncertainties in the short-range contribution.

It is important to note that such a “wrong-sign” spin-orbit interaction from iterated one-pion exchange (entirely through

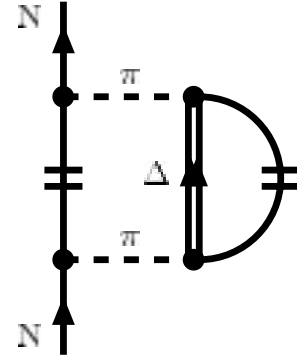


FIG. 4. Three-body diagram of two-pion exchange with virtual  $\Delta(1232)$ -isobar excitation. For a nucleon it generates a sizeable three-body spin-orbit force of the “right sign.” The horizontal double lines symbolize the filled Fermi sea of nucleons. The analogous diagram does not exist for a  $\Lambda$  hyperon.

the second-order tensor force) exists indeed also for nucleons (see Fig. 4 in Ref. [27]).\* It has, however, been found recently that three-body spin-orbit forces generated by  $2\pi$ -exchange with virtual  $\Delta(1232)$ -isobar excitation compensate this contribution to a large extent [28] (see Fig. 2 therein), leaving all room for additional short-distance contributions. In the case of the  $\Lambda$ -hyperon the analogous three-body effects with virtual  $\Delta(1232)$ -isobar excitation are not possible and therefore the sizeable “wrong-sign” spin-orbit interaction generated by iterated pion-exchange becomes visible. The absence of analogous three-body mechanisms for the  $\Lambda$ -hyperon becomes immediately clear by inspection of the relevant  $2\pi$ -exchange diagram in Fig. 4. Replacing the external nucleon by a  $\Lambda$  hyperon introduces as the intermediate state on the open baryon line a  $\Sigma$  hyperon for which there exists no filled Fermi sea. The so-far emerging picture of the nuclear spin-orbit interaction is a rather intriguing one. The spin-orbit coupling of nucleons in nuclei is predominantly of short-range origin because the long-range  $2\pi$ -exchange components find a mechanism of self-cancellation. The smallness of the  $\Lambda$ -nuclear spin-orbit coupling, conversely, reveals the existence of a long-range  $2\pi$ -exchange component of the “wrong sign.”

#### IV. CONCLUDING REMARKS

In summary we have calculated the density-dependent  $\Lambda$ -nuclear mean-field  $U_\Lambda(k_f)$  in the framework of SU(3) chiral perturbation theory. The leading order contributions emerge from kaon-exchange and iterated pion exchange with  $\Sigma$  hyperons in the intermediate state. The empirical potential depth  $U_\Lambda(k_{f0}) \simeq -28 \text{ MeV}$  is well reproduced with a cutoff

\*One should note, however, that the one-pion exchange tensor force is too strong at intermediate and short distances, so that its effect on the spin-orbit coupling, as calculated in this work, represents an upper limit in magnitude.

scale  $\bar{\Lambda} = 0.70$  GeV, equivalent to a contact interaction, which represents effectively all short-range dynamics not “resolved” at scales characteristic of the nuclear Fermi momentum. The anomalously small  $\Lambda$ -nuclear spin-orbit interaction finds a novel and natural explanation in terms of the strong cancellation between short-range contributions (roughly estimated from the empirical nucleonic spin-orbit coupling strength, admittedly with large uncertainties) and long-range contributions generated by iterated pion-exchange with  $\Sigma$  hyperons in the intermediate state. The exceptionally small  $\Sigma\Lambda$ -mass

splitting  $M_{\Sigma} - M_{\Lambda} = 77.5$  MeV prominently influences the long-range iterated  $1\pi$ -exchange effects.

### ACKNOWLEDGMENTS

We thank R. Furnstahl, A. Gal, and G. Lalazissis for informative discussions. This research is part of the EU integrated infrastructure initiative hadron physics project under contract number R113-CT-2004-506078. This work was also supported in part by BMBF and GSI.

- 
- [1] R. E. Chrien and C. B. Dover, *Ann. Rev. Nucl. Part. Sci.* **39**, 113 (1989), and references therein.
  - [2] D. J. Millener, C. B. Dover, and A. Gal, *Phys. Rev. C* **38**, 2700 (1988).
  - [3] H. Bando *et al.*, *Prog. Theor. Phys. (Suppl.)* **81**, 1–203 (1985), and references therein.
  - [4] H. Bando, T. Motoba, and J. Zofka, *Int. J. Mod. Phys. A* **21**, 4021 (1990).
  - [5] S. Ajimura *et al.*, *Phys. Rev. Lett.* **86**, 4255 (2001).
  - [6] R. Brockmann and W. Weise, *Phys. Lett.* **B69**, 167 (1977); J. V. Noble, *Phys. Lett.* **B89**, 325 (1980).
  - [7] H. J. Pirner, *Phys. Lett.* **B85**, 190 (1979).
  - [8] B. K. Jennings, *Phys. Lett.* **B246**, 325 (1990); E. D. Cooper, B. K. Jennings, and J. Mares, *Nucl. Phys.* **A580**, 419 (1994).
  - [9] T. A. Rijken, V. G. J. Stoks, and Y. Yamamoto, *Phys. Rev. C* **59**, 21 (1999).
  - [10] C. B. Dover and A. Gal, *Prog. Part. Nucl. Phys.* **12**, 171 (1984).
  - [11] E. Hiyama, *Phys. Rev. Lett.* **85**, 270 (2000).
  - [12] D. J. Millener, *Nucl. Phys.* **A691**, 93c (2001); *nucl-th/0402091*.
  - [13] P. Papazoglou *et al.*, *Phys. Rev. C* **59**, 411 (1999).
  - [14] H. Müller and J. R. Shepard, *J. Phys. G* **26**, 1049 (2000).
  - [15] K. Tsushima, K. Saito, J. Haidenbauer, and A. W. Thomas, *Nucl. Phys.* **A630**, 691 (1998).
  - [16] Y. Fujiwara, M. Kohno, T. Fujita, C. Nakamoto, and Y. Suzuki, *Nucl. Phys.* **A674**, 493 (2000).
  - [17] O. Dumbrajs *et al.*, *Nucl. Phys.* **B216**, 277 (1983).
  - [18] I. J. General and S. R. Cotanch, *Phys. Rev. C* **69**, 035202 (2004).
  - [19] B. Loiseau and S. Wycech, *Phys. Rev. C* **63**, 034003 (2001).
  - [20] N. Kaiser, R. Brockmann, and W. Weise, *Nucl. Phys.* **A625**, 758 (1997).
  - [21] N. Kaiser, S. Fritsch, and W. Weise, *Nucl. Phys.* **A697**, 255 (2002); *nucl-th/0406038*, *Nucl. Phys. A* (2005) (to be published), and references therein.
  - [22] N. Kaiser, *Nucl. Phys.* **A709**, 251 (2002).
  - [23] X. Jin and R. J. Furnstahl, *Phys. Rev. C* **49**, 1190 (1994).
  - [24] P. Finelli, N. Kaiser, D. Vretenar, and W. Weise, *Eur. Phys. J. A* **17**, 573 (2003); *Nucl. Phys.* **A735**, 449 (2004), and references therein.
  - [25] A. Bohr and B.R. Mottelson, *Nuclear Structure*, Vol. I, (Benjamin, New York, 1969).
  - [26] E. Chabanat, P. Bonche, P. Haensel, J. Meyer, and R. Schaeffer, *Nucl. Phys.* **A635**, 231 (1998).
  - [27] N. Kaiser, S. Fritsch, and W. Weise, *Nucl. Phys.* **A724**, 47 (2003).
  - [28] N. Kaiser, *Phys. Rev. C* **68**, 054001 (2003).